Available online at www.sciencedirect.com

SciVerse ScienceDirect

Ceramics International 39 (2013) 1971–1976

CERAMICS INTERNATIONAL

www.elsevier.com/locate/ceramint

Influence of Sr/Ba ratio on the dielectric, ferroelectric and pyroelectric properties of strontium barium niobate ceramics

Jing Zhang, Genshui Wang*, Feng Gao, Chaoliang Mao, Fei Cao, Xianlin Dong

Key Laboratory of Inorganic Functional Materials and Devices, Shanghai Institute of Ceramics, Chinese Academy of Sciences, 1295 Dingxi Road, Shanghai 200050, People's Republic of China

Received 24 June 2012; received in revised form 16 August 2012; accepted 16 August 2012
Available online 23 August 2012

Abstract

$Sr_xBa_{1-x}Nb_2O_6$ (with $x=0.50$, 0.45, 0.40 and 0.30) ceramics were synthesized by conventional solid-state method and sintered at 1350 °C for 3 h. The phase structure, microstructure, dielectric, ferroelectric and pyroelectric properties of obtained ceramics were systematically investigated. Pure tungsten bronze phase could be obtained in all ceramics. The dielectric characteristics showed that SBN ceramic was a relaxor with strong diffuse phase transition and weak frequency dispersion. As Sr molar fraction x increases from 0.30 to 0.50, the transition temperature T_C decreased linearly while the diffusivity parameter γ declined from 1.88 to 1.68. The saturated polarization, remnant polarization and pyroelectric coefficient were also found to be enhanced in SBN ceramics with increasing Sr content. The pyroelectric coefficient of about 2×10^{-8} C/cm^{2}K can be obtained for polarized SBN50 ceramics at room temperature.
© 2012 Elsevier Ltd and Techna Group S.r.l. All rights reserved.

Keywords: C. Dielectric dispersion; D. Lead-free ceramics; Pyroelectric properties; Strontium barium niobate

1. Introduction

Pyroelectric infrared detectors have been of interest for many years because of their broad wavelength response, room-temperature operation, high stability and good sensitivity over a wide temperature range [1,2]. Ferroelectric ceramics widely used in pyroelectric infrared detectors are mainly lead-based ceramics such as lead titanate (PT)-based [3], lead zirconate titanate (PZT)-based [4] and lead magnoniobate (PMN)-based [5] due to their superior pyroelectric properties. However, the toxicity of lead-based materials either during the manufacturing process (evaporation of lead) or after making the device is of serious concerns. Therefore, developing lead-free ceramics for replacing the lead-containing ceramics is greatly needed in various applications.

For the past few years several systems of lead-free materials, such as bismuth sodium titanate (BNT)-based [6], potassium sodium niobate (KNN)-based [7] and strontium barium niobate (SBN)-based [8,9] have been reported for pyroelectric applications. Among them SBN crystals [10,11] and textured ceramics [8] have been reported to have excellent pyroelectric propertied comparable to PZT ceramics.

SBN ($Sr_xBa_{1-x}Nb_2O_6$) has an open tetragonal tungsten bronze (TTB) structure consisting of ten NbO_6 octahedra linked by corners [12]. Most of the physical properties of SBN, such as ferroelectric, pyroelectric and electro-optic, can be altered by modifying its composition [13,14]. A.M. Glass [13] got very different dielectric and pyroelectric properties in SBN single crystals by varying Sr/Ba ratio. Nevertheless, most of these studies were confined in single crystals. Generally, ceramic is more widely used than single crystal for its low cost and easy fabrication. However, a systematic research about the effect of Sr/Ba ratio on the dielectric, ferroelectric and pyroelectric properties of SBN ceramics has not been reported yet.

In this work, the phase transition characteristics of SBN ceramics with different Sr/Ba ratios were investigated by dielectric measurements. The ferroelectric and pyroelectric properties of SBN ceramics were also studied to

*Corresponding author.
E-mail address: genshuiwang@mail.sic.ac.cn (G. Wang).

0272-8842/$ - see front matter © 2012 Elsevier Ltd and Techna Group S.r.l. All rights reserved.
http://dx.doi.org/10.1016/j.ceramint.2012.08.048

evaluate its potential for applications in uncooled infrared detectors.

2. Experimental procedure

The $Sr_xBa_{1-x}Nb_2O_6$ bulk ceramics were prepared by a traditional solid-state ceramic fabrication method. The compositions discussed in this article were prepared according to the formulas presented in Table 1. The starting raw materials $BaCO_3$ (99%), $SrCO_3$ (99%) and Nb_2O_5 (99.5%) were ball-milled for 24 h in ethanol. The mixture was dried, calcined at 1200 °C for 3 h and then ball-milled again for 48 h. The powders were compacted into green disks with a diameter of 15 mm under 100 MPa. The dielectric properties and microstructures of SBN50 sintered at 1300 °C, 1350 °C and 1400 °C were investigated to confirm the sintering condition. All samples were sintered in air at 1350 °C for 3 h according to the results.

The crystal structure of the ceramics was characterized by powder x-ray diffraction (XRD, D/MAX-2550 V; Rigaku, Tokyo, Japan). Patterns were recorded on sintered powders. The microstructure of the ceramics was taken by scanning electron microscope (SEM, JSM-6700F, JEOL, Japan) on the polished and heat-etched sample surface. Electric measurements were carried out after the samples were polished to 0.5 mm in thickness and coated with silver electrode on both sides. The dielectric constant (ε_r) and dissipation factor ($\tan\delta$) of unpolarized samples were measured using a Hewlett Packard LCR meter at different frequencies in a temperature range from 20 °C to 200 °C. The polarization versus electric field (*P–E*) hysteresis loops were characterized by aixACCT TF Analyzer 2000 (aixACCT Systems GmbH; Dennewartstrasse, Aachen, Germany) with high-voltage power supply (Trek Inc., Medina, NY). A sinusoidal waveform was chosen for the electric field cycle. The pyroelectric properties were studied with a Keithley 6517A electrometer/high resistance meter for polarized samples. The poling electric fields were determined according to the *P–E* hysteresis loops and the samples were polarized in silicone oil under an electric field of 5 kV/mm at 150 °C for 60 min and then cooled down until 40 °C with the electric field maintained at 5 kV/mm, similar as the reported poling progress for SBN relaxor [8].

Table 1
Compositions with varying Sr/Ba ratios of SBN ceramics.

Sample	Composition
SBN50	$Sr_{0.50}Ba_{0.50}Nb_2O_6$
SBN45	$Sr_{0.45}Ba_{0.55}Nb_2O_6$
SBN40	$Sr_{0.40}Ba_{0.60}Nb_2O_6$
SBN30	$Sr_{0.30}Ba_{0.70}Nb_2O_6$

3. Results and discussion

3.1. Phase and microstructure

Fig. 1 shows the XRD patterns of SBN ceramics sintered at 1350 °C for 3 h. All the diffraction peaks can be ascribed to the crystalline TTB phase, which indicates that the samples are crystallized into a pure TTB structure without second phase.

The surface microstructures of SBN ceramics sintered at the same temperature of 1350 °C are shown in Fig. 2(a)–(d). All the samples are observed to exhibit well grown grains and clear crystalline boundaries, with an average grain size of about 1–3 μm. Further measurement indicates the density of SBN series samples all reaches 94% of the theoretical value. The theoretical density for each composition is calculated from XRD analysis. Sintering at the same temperature of 1350 °C for 3 h probably causes the grain size of SBN ceramics not to present an obvious change as the Sr/Ba ratio decreases.

3.2. Dielectric and phase transition properties

Fig. 3 shows the temperature-dependent dielectric constant (ε_r) of SBN ceramics in different compositions measured at 100 Hz, 1 kHz, 10 kHz, 100 kHz and 1 MHz. Diffuse phase transition (DPT), frequency-dependent T_C and dielectric dispersion were observed in all the SBN samples. The broadening of the phase transition may be due to structural disorder and compositional fluctuations in the solid solution [15,16]. It is also believed that the origin of the relaxor behavior in SBN is due to electric random fields (RFs) which promote the formation of short-range ordered polar nanoregions (PNRs). RFs are thought to relate to randomly distributed vacancies on A sites of the unfilled TTB structure of the stoichiometric SBN [12]. It has been widely reported in SBN systems

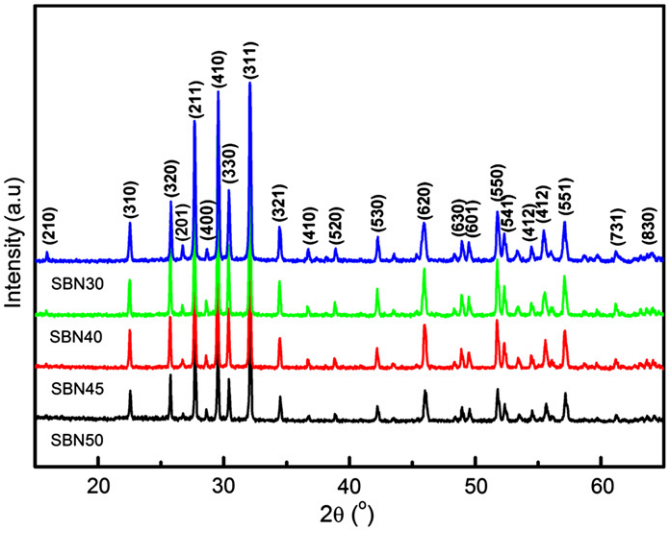

Fig. 1. The X-ray diffraction patterns of SBN ceramics.

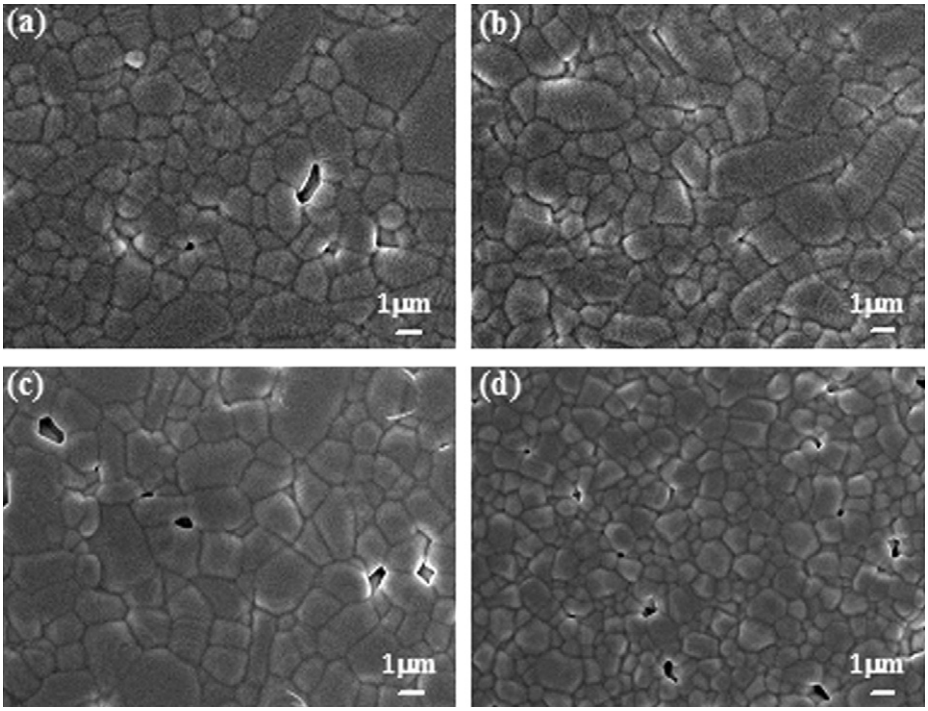

Fig. 2. SEM micrographs of SBN ceramics: (a) SBN50, (b) SBN45, (c) SBN40 and (d) SBN30.

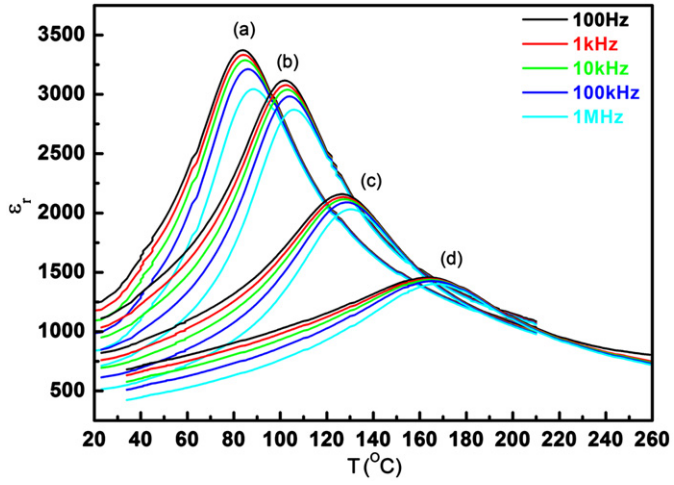

Fig. 3. Dielectric constant (ε_r) of SBN ceramics as a function of temperature for composition: (a) SBN50, (b) SBN45, (c) SBN40 and (d) SBN30.

that the inherent RFs and PNRs result in relaxor type of dielectric characteristics, including broaden phase transition region [17], significant frequency dependence of the peak permittivity [18] and notable aging effects [19]. The important dielectric phase transition parameters for all the four samples are listed in Table 2. The Curie temperature (T_C) is defined as the temperature of maximum dielectric constant (ε_m) at 1 kHz. The value of T_C decreases from 164 °C to 84 °C while ε_m at 1 kHz rises from 1445 to 3332 as Sr/Ba ratio increases from 3/7 to 1/1. The ferroelectric ordering temperature (T_C) is determined by the competition between RFs and correlation

Table 2
Dielectric parameters for Sr_xBa_{1-x} Nb_2O_6 ceramics of different compositions.

Parameters	Samples			
	SBN50	SBN45	SBN40	SBN30
ε_m (1 kHz)	3332	3076	2134	1445
T_C or T_m (1 kHz)/°C	84	102	127	164
$T_{0.9\varepsilon m}$ (1 kHz)/°C	96	115	142	185
T_m (100 Hz)/°C	84	102	126	163
T_m (1 MHz)/°C	88	105	130	166
ΔT_{relax}/°C	4	3	4	3
$\Delta T_{diffuse}$ (1 kHz)/°C	12	13	15	21
γ (1 kHz)	1.68	1.73	1.78	1.88

between PNRs in ceramics [15]. The former would suppress but the latter would enhance T_C. The T_C decrease in SBN ceramics can be ascribed to the fact that more Sr (smaller than Ba) ions within the open TTB crystal structure give rise to enhanced polar disorder which would increase RFs and thus decrease T_C. Shvartsman et al. [20] studied SBN crystals with piezoresponse force microscopy (PFM) and draw the similar conclusion. In addition, the correlation between PNRs can be remarkably depressed at high temperature as a result of enhanced disorder [15,21]. In view of the fact that the dielectric constant at T_C (ε_m) is determined by the magnitude of the dipole moment of PNRs and the strength of the correlation between PNRs basically is determined by their dipole moments [15], the decrease of ε_m from SBN50 to SBN30 may be due to the weakening of the correlation between PNRs around their peak temperatures.

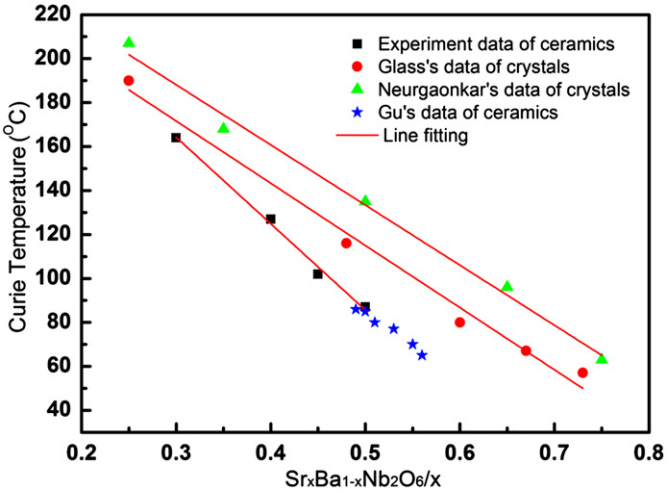

Fig. 4. Curie temperature (T_C) of SBN ceramics measured at 1 kHz as a function of Sr molar fraction (x). The values for SBN found in the literature are also included for comparision: (●) Ref. [13], (▲) Ref. [23] and (★) Ref. [22].

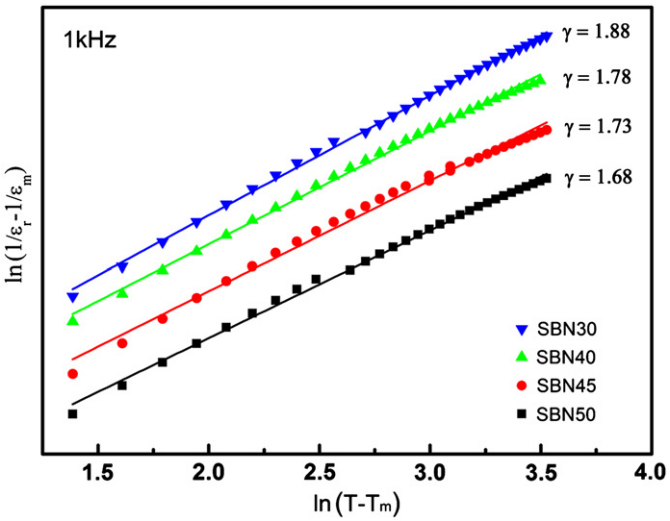

Fig. 5. Variation of $\ln(1/\varepsilon_r - 1/\varepsilon_m)$ with $\ln(T - T_m)$ at 1 kHz for different compositions.

The T_C values of SBN with different Sr content measured at 1 kHz are shown in Fig. 4. A linear relation of T_C with Sr molar fraction x occurs for $0.3 \le x \le 0.5$ is observed. From this linearity, the T_C of the $Sr_xBa_{1-x}Nb_2O_6$ (SBN) system with other Sr molar fraction x can be designed by controlling the Sr fraction, and an empirical equation can be obtained for $0.3 \le x \le 0.5$:

$$T_C(^oC) = 286 - 405x \quad (1)$$

where x is the Sr molar fraction. The asterisks (★) in Fig. 4 are the T_C values of SBN ceramics at 1 kHz for different compositions reported by Gu [22], which fit well with the linear relation we define. The reported values of T_C for SBN single crystals are also shown in Fig. 4 and similar linear relation of T_C versus composition can be observed in SBN crystals. The works of Neurgaonkar [23] and Glass [13] also indicate that the SBN single crystals always have higher T_C than ceramics for the same composition. This decrease of T_C in ceramics may be attributed to enhanced polar disorder in ceramics. The large amounts of grain boundaries in ceramic promote the formation of short-range ordered polar nanoregions (PNRs), which decrease the ferroelectric ordering temperature.

It is known that the dielectric characteristics of relaxor ferroelectrics deviate from the typical Curie–Weiss behavior and can be described by the Uchino and Nomura function, a modified Curie–Weiss relationship [24]:

$$\frac{1}{\varepsilon_r} - \frac{1}{\varepsilon_m} = \frac{(T - T_m)^\gamma}{C}, \quad 1 \le \gamma \le 2 \quad (2)$$

where ε_m is the maximum value of dielectric constant, ε_r is the dielectric constant at temperature T, T_m is the temperature at the peak of the dielectric constant, C is the Curie constant, and γ is the diffusivity parameter, taking the value between 1 (for normal ferroelectrics) and 2 (for a complete DPT). Thus the value of γ can also be used to characterize the relaxor behavior.

In order to further confirm the effects of Sr/Ba ratio on the relaxor feature of SBN ceramics, the plots of $\ln(1/\varepsilon_r - 1/\varepsilon_m)$ as a function of $\ln(T - T_m)$ have been made for SBN samples with different Sr content at 1 kHz, which are shown in Fig. 5. The slope of the fitting curves is used to determine the γ value. It can be seen that γ values of all samples are close to 2, so the phase transitions in all SBN ceramics exhibit a obvious diffuse characteristic. The diffuseness of the phase transition is composition dependent and shows considerable enhancement with higher Sr content. In consideration of the fact that SBN ceramics with more Sr have higher T_C and the strength of the correlation of PNRs can be suppressed markedly at high temperature, the polar disorder in the vicinity of T_C would be strengthened as Sr content increases. Thus the phase transition becomes more diffused.

In addition, the parameters of ΔT_{relax} and $\Delta T_{diffuse}$ (1 kHz) were introduced to investigate the relaxor feature of SBN. The specific symbols of the relaxation degree and the diffuseness degree are defined as [25]:

$$\Delta T_{relax} = T_m(1\ \text{MHz}) - T_m(100\ \text{Hz}) \quad (3)$$

$$\Delta T_{diffuse}(1\ \text{kHz}) = T_{0.9\varepsilon_m}(1\ \text{kHz}) - T_m(1\ \text{kHz}) \quad (4)$$

Based on the experimental data, the values of ΔT_{relax} and $\Delta T_{diffuse}$ (1 kHz) were calculated and are listed in Table 2. We can see that with increasing Sr content, $\Delta T_{diffuse}$ (1 kHz) declines remarkably but ΔT_{relax} keep low and shift little. All the empirical parameters above suggest that the SBN ceramic is indeed a relaxor with strong DPT and weak frequency dispersion. David et al. [26] reported that on increase of the Sr/Ba ratio a transformation from ferroelectric to relaxor takes place in SBN single crystal. However, our results reveal that this transformation can be depressed in SBN ceramics. The enhanced relaxation stability with composition in SBN ceramics is probably attributed to the grain boundary

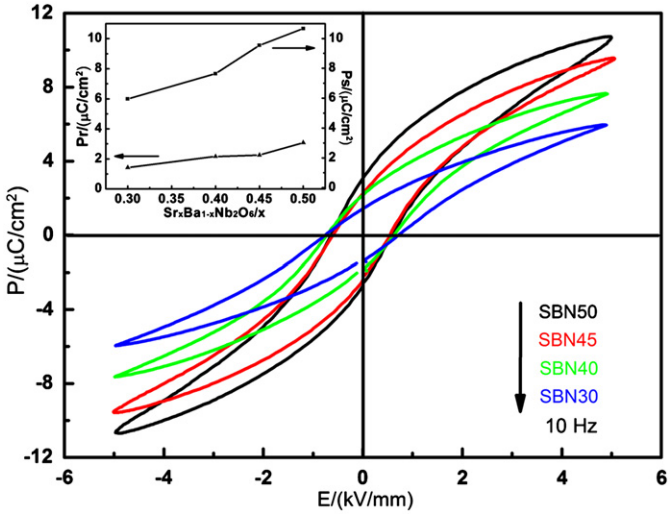

Fig. 6. The *P–E* hysteresis loops of SBN ceramics measured at 10 Hz and the inset shows the dependence of *Ps* and *Pr* on the Sr/Ba ratio.

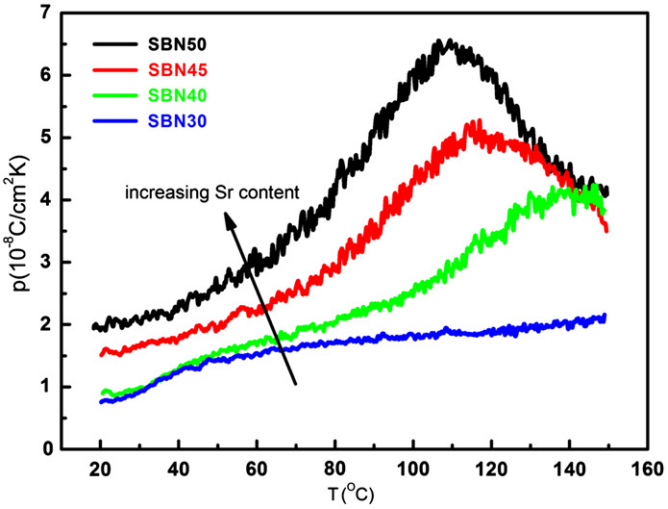

Fig. 7. Pyroelectric coefficient (*p*) of SBN ceramics as a function of temperature for different compositions.

effect which weaken the influence of RFs on the relaxation by releasing stress.

3.3. Ferroelectric and pyroelectric properties

Fig. 6 shows the polarization versus applied electrical field (*P–E*) hysteresis loops of SBN ceramics for different compositions measured under 5 kV/mm at room temperature. It can be observed that the room temperature values of saturated polarization *Ps* and remnant polarization *Pr* both increase monotonically with increasing Sr content over the entire range of composition investigated, reaching 10.66 μC/cm^2 and 3.08 μC/cm^2 for SBN50 under 5 kV/mm, respectively. This ferroelectricity is comparable to that published for SBN50 ceramic [9,27]. The increment of *Ps* with Sr content may owe to the higher dielectric constant at room temperature, as shown in Fig. 3. SBN samples with larger Sr content are found to have lower coercive field as a result of lower T_C, which also make it easier for them to be polarized hence have higher values of *Pr*.

The pyroelectric coefficient is one of the most important parameters for pyroelectric device applications. The pyroelectric coefficient (*p*) of SBN ceramics as a function of temperature for all compositions is shown in Fig. 7. The value of *p* at room temperature is about 2×10^{-8} C/cm^2 K for SBN50. This result is lower than that of single crystal [11] but four times higher than the earlier reports for SBN50 ceramics [9]. In ceramics, the grains orientate randomly and this random orientation decreases the effective polarization, thus suppressing the measured pyroelectric coefficient. The data also reveals that the pyroelectric coefficient of SBN ceramics decrease while the temperature dependence of pyroelectric properties becomes weaker with reduced Sr content. As continuous changes occured in dielectric and ferroelectric properties while no remarkable difference was observed in phase and microstructure of SBN ceramics for various compositions, the decrease of *p* should mainly be attributed to Sr/Ba ratio variations that shifted T_C significantly from ~84 to ~164 °C and simultaneously suppressed *Pr*. With decreasing Sr content, *Pr* of SBN ceramics decreases from lower values towards zero over a wider temperature range, resulting in lower pyroelectric coefficient.

4. Conclusion

Pure tetragonal tungsten bronze phase $Sr_xBa_{1-x}Nb_2O_6$ (with $x=0.50$, 0.45, 0.40 and 0.30) ceramics were obtained and their microstructure, dielectric, ferroelectric and pyroelectric properties were systematic investigated. The dielectric characteristics showed that SBN ceramic was a relaxor with strong diffuse phase transition and weak frequency dispersion. As Sr molar fraction *x* increases from 0.30 to 0.50, the transition temperature T_C decreased linearly and the diffusivity parameter γ declined from 1.88 to 1.68. Normal ferroelectric hysteresis loops could be observed in all compositions. The saturated polarization, remnant polarization and pyroelectric coefficient were also found to be enhanced in SBN ceramics with increasing Sr content. Relatively large and stable pyroelectric coefficient of about 2×10^{-8} C/cm^{2}K could be obtained in SBN50 ceramics, unveiling its potential for applications in uncooled infrared detectors.

Acknowledgments

This work was supported by the National Program on Key Basic Research Project (973 Program) (Grant no. 2012CB619406) and the Shanghai Key Projects of Basic Research (10DJ1400203).

References

[1] M.H. Lee, R. Guo, A.S. Bhalla, Pyroelectric sensors, Journal of Electroceramics 2 (4) (1998) 229–242.

[2] R.W. Whatmore, P.C. Osbond, N.M. Shorrocks, Ferroelectric materials for thermal IR detectors, Ferroelectrics 76 (1) (1987) 351–367.
[3] R.W. Whatmore, A.J. Bell, Pyroelectric ceramics in the lead zirconate–lead titanate–lead iron niobate system, Ferroelectrics 35 (1–4) (1981) 155–160.
[4] J. Lian, T. Shiosaki, Pyroelectric properties of Pb[Zr,Ti,(Zn,Nb)]O_3 solid solution ceramics, Ferroelectrics 118 (1) (1991) 135–141.
[5] P. Kumar, S. Sharma, O.P. Thakur, C. Prakash, T.C. Goel, Dielectric, piezoelectric and pyroelectric properties of PMN–PT (68:32) system, Ceramics International 30 (4) (2004) 585–589.
[6] S.T. Lau, C. Cheng, S. Choy, D. Lin, K. Kwok, H.L.W. Chan, Lead-free ceramics for pyroelectric applications, Journal of Applied Physics 103 (10) (2008) 104105.
[7] S.B. Lang, Guide to the literature of piezoelectricity and pyroelectricity. 25, Ferroelectrics 330 (1) (2006) 103–182.
[8] M. Venet, I.A. Santos, J.A. Eiras, D. Garcia, Potentiality of SBN textured ceramics for pyroelectric applications, Solid State Ionics 177 (5–6) (2006) 589–593.
[9] Y. Yao, C.L. Mak, K.H. Wong, S. Lu, Z. Xu, Effects of rare earth dopants on the ferroelectric and pyroelectric properties of strontium barium niobate ceramics, International Journal of Applied Ceramic Technology 6 (6) (2009) 671–678.
[10] A.M. Glass, Ferroelectric $Sr_{1-x}Ba_xNb_2O_6$ as a fast and sensitive detector of infrared radiation, Applied Physics Letters 13 (4) (1968) 147–149.
[11] J.C. Joshi, A.L. Dawar, Pyroelectric materials, their properties and applications, Physica Status Solidi A 70 (2) (1982) 353–369.
[12] W. Kleemann, J. Dec, P. Lehnen, R. Blinc, B. Zalar, R. Pankrath, Uniaxial relaxor rerroelectrics: the ferroic random-field Ising model materialized at last, Europhysics Letters 57 (2002) 14.
[13] A.M. Glass, Investigation of the electrical properties of $Sr_{1-x}Ba_xNb_2O_6$ with special reference to pyroelectric detection, Journal of Applied Physics 40 (12) (1969) 4699–4713.
[14] P.V. Lenzo, E.G. Spencer, A.A. Ballman, Electro-optic coefficients of ferroelectric strontium barium niobate, Applied Physics Letters 11 (1) (1967) 23–24.
[15] T.T. Fang, H.Y. Chung, Dielectric relaxation behavior of undoped, Ce-, and Cr-doped $Sr_{0.5}Ba_{0.5}Nb_2O_6$ at high temperatures, Applied Physics Letters 94 (9) (2009) 092905.
[16] M.E. Lines, A.M. Glass, Principles and Applications of Ferroelectrics and Related Materials, Oxford University Press, Oxford, 1977.
[17] I.A. Santos, D.U. Spinola, D. Garcia, J.A. Eiras, Dielectric behavior and diffuse phase transition features of rare earth doped $Sr_{0.61}Ba_{0.39}Nb_2O_6$ ferroelectric ceramics, Journal of Applied Physics 92 (6) (2002) 3251–3256.
[18] J. Banys, J. Macutkevic, R. Grigalaitis, W. Kleemann, Dynamics of nanoscale polar regions and critical behavior of the uniaxial relaxor $Sr_{0.61}Ba_{0.39}Nb_2O_6$:Co, Physical Review B 72 (2) (2005) 024106.
[19] L.K. Chao, E.V. Colla, M.B. Weissman, D.D. Viehland, Aging and slow dynamics in $Sr_xBa_{1-x}Nb_2O_6$, Physical Review B 72 (13) (2005) 134105.
[20] V.V. Shvartsman, W. Kleemann, T. Łukasiewicz, J. Dec, Nanopolar structure in $Sr_xBa_{1-x}Nb_2O_6$ single crystals tuned by Sr/Ba ratio and investigated by piezoelectric force microscopy, Physical Review B 77 (5) (2008) 054105.
[21] H. Rosenfeld, T. Egami, A model of short and intermediate range atomic structure in the relaxor ferroelectric Pb ($Mg_{1/3}$, $Nb_{2/3}$) O_3, Ferroelectrics 158 (1) (1994) 351–356.
[22] R. Gu, Fabrication and Characterization of SBN Based Ceramics, in: Proceedings of the Inorganic Chemistry, vol. Master Dissertation, Shangxi Normal University, Shangxi, 2010.
[23] R.R. Neurgaonkar, W.F. Hall, J.R. Oliver, W.W. Ho, W.K. Cory, Tungsten bronze $Sr_{1-x}Ba_xNb_2O_6$: a case history of versatility, Ferroelectrics 87 (1) (1988) 167–179.
[24] K. Uchino, S. Nomura, Critical exponents of the dielectric constants in diffused-phase-transition crystals, Ferroelectrics 44 (1) (1982) 55–61.
[25] L. Cui, Y.D. Hou, S. Wang, C. Wang, M.K. Zhu, Relaxor behavior of (Ba,Bi)(Ti,Al)O_3 ferroelectric ceramic, Journal of Applied Physics 107 (5) (2010) 054105.
[26] C. David, T. Granzow, A. Tunyagi, M. Wöhlecke, T. Woike, K. Betzler, M. Ulex, M. Imlau, R. Pankrath, Composition dependence of the phase transition temperature in $Sr_xBa_{1-x}Nb_2O_6$, Physica Status Solidi A 201 (8) (2004) R49–R52.
[27] P.K. Patro, A.R. Kulkarni, C.S. Harendranath, Dielectric and ferroelectric behavior of SBN50 synthesized by solid-state route using different precursors, Ceramics International 30 (7) (2004) 1405–1409.